Stanford Exploration Project, Report 112, November 11, 2002, pages 259–??

Exploring the relationship between uncertainty of AVA attributes and rock information

Weitian Chen and Robert Clapp[1]

ABSTRACT

Amplitude versus Angle (AVA) attributes include information about rock properties. Using a dataset from South America, we performed a multiple realization method to get multiple equal-probable AVA intercepts, gradients, and their products. We generated a 3-D histogram to evaluate the variability of those AVA attributes. In the same area, we chose a 2-D section by matching it to three wells. Then we calculated the shale volume along these three wells and found the well with low shale volume has high AVA uncertainty, which made us guess the low shale/sand ratio may cause high AVA uncertainty. The further work need to be done is to use more real data to exam our conjecture, namely, whether there exist an empirical relationship between AVA uncertainty and rock information, such as shale volume, impedance or velocity.

INTRODUCTION

Uncertainty is an inherent problem existing in velocity analysis. It is important for geophysicists to assess the variability of the velocity quantitatively. As an alternative to a common geostatistical method (Isaaks and Srivastava, 1989), Clapp (2000; 2001) introduced multiple realization method for complex operators. Clapp modified the standard geophysical inversion technique by adding random noise into the model styling goal to achieve multiple realizations. By comparing and contrasting the equal-probable realizations, the variability can be evaluated. Since the subsurface image is obtained based on the new velocity model, the uncertainty of velocity model will cause the uncertainty of amplitude information we can acquired from image (Mora and Biondi, 2000). Using the multiple realization method, Clapp (2002) showed how the velocity uncertainty affected the amplitude information.

Amplitudes carry important information about rock properties. Amplitude variation with offset (AVO) is a widely used technique in petroleum industry because AVO anomalies often indicates hydrocarbon existence. A good review of AVO analysis is provided by Castagna (1993a). Since AVO is dependent on intrinsic rock parameters such as compressional-wave velocity, shear-wave velocity, density, anisotropy and attenuation, AVO can be used to assess information for rock properties, such as lithology, porosity and pore fluid content. Castagna (1993b) provide a rock physics framework for AVO analysis.

[1]**email:** chen@sep.stanford.edu, bob@sep.stanford.edu

The relationship between AVO and rock properties make us guess there may exist empirical relationships between AVO uncertainty and rock information. For example, if we get high variance of AVO attributes (which can be evaluated from multiple realizations) at specific subsurface areas, we can conjecture that there may be some change in rock information in the same area, such as impedance, velocity or shale/sand ratio. In this paper, we explored such relationships.

Instead of extracting amplitude variations with offset, we adopted amplitude variation with angle (AVA) analysis because realistic velocities usually break the simple relationship between offset and angle. The dataset we used was from South America. We evaluated the variability of AVA attributes by using a 3-D histogram. A 2-D section was extracted and shale volume along the wells in this section were calculated. We found the well with low shale volume has obvious higher AVA uncertainty than other two wells, which made us conjecture the low shale/sand ratio will cause high AVA uncertainty. The further work need to be done is to use more real data to exam whether our guess is true or there exist other empirical relationships between AVA uncertainty and rock information, such as shale volume, impedance or velocity.

METHODOLOGY TO EVALUATE THE UNCERTAINTY OF AVA ATTRIBUTES

We will use multiple equal-probable velocity models to get multiple images. From those images, we can extract angle gathers and get intercept A and slope B (Gratwick, 2001). By comparing and contrasting the multiple realizations of these AVA attributes, we can access their variability.

Using multiple realization method to get multiple equal-probable velocity models

Regularized geophysical inversion problems include two fitting goals: data fitting and model styling. They can be written as:

$$0 \approx \mathbf{r_d} = \mathbf{d} - \mathbf{Lm} \tag{1}$$

$$0 \approx \mathbf{r_m} = \epsilon \mathbf{Am} \tag{2}$$

An ideal regularization operator **A** should be the inverse model covariance. In practice, according to the difficulty to get the explicit model covariance, **A** is usually approximated as Lapacian, PEF or steering filter.

Generally, the regularization operator only describes the two point statistics. The first order statistics, spatial variance, is not included in it. Like in geostatistics, we can add normal noise vector $\boldsymbol{\eta}$ into model styling goal so that we can get the comparable variance in poorly determined regions as in well determined regions (Claerbout, 1999; Clapp, 2000).

The fitting goals including both first and second model statistics can be written as:

$$0 \approx \mathbf{r_d} = \mathbf{d} - \mathbf{Lm} \tag{3}$$

$$\sigma_m \boldsymbol{\eta} \approx \mathbf{r_m} = \epsilon \mathbf{Am} \tag{4}$$

Scalar σ_m can be approximated as the variance of the model residual acquired by applying regularization operator $\mathbf{A}$ to first estimated model (Claerbout, 1999). By changing normal noise $\boldsymbol{\eta}$, we can get equal-probable models from which we can evaluate the variability of the model.

When we perform velocity analysis, the data we used are the value picked from semblance. So there also exist data uncertainty. Similar to the modification of model styling goal, we can add normal noise into the data fitting goal in terms of noise covariance to include this effect on our model evaluation. The noise inverse covariance can be approximated as the chain of a diagonal operator and a PEF on $\mathbf{r}_d$. A detailed discussion on how to include data and model uncertainty to evaluate velocity was given by Clapp (2002).

Amplitude Balance

During a seismic survey, it can't be guaranteed that all the receivers have the same response. Neither can we promise that the energy for all shots have same energy. So, the recorded amplitude difference between traces will include not only rock information but also artifacts caused by different sources and receivers. We should remove such artifacts before performing AVA analysis.

For each trace, its amplitude square A_t can be expressed as

$$A_t = R_t S_t G_t U_t \tag{5}$$

Here, R_t is the component from the unique receiver the trace is corresponding to; S_t is from the unique source the trace is corresponding to; G_t corresponding to geometrical spreading for this trace; and U_t is the remaining amplitude component which contains the information related to rock properties. The way we balanced the amplitude is the following:

1. Extract the same depth window for all traces and calculate the sum of the amplitude square for all traces in this window.
2. Using the conjugate gradient method to solve for R_t, S_t, G_t and U_t using (5).
3. The problem will be underdetermined. We regularize the problem by applying Laplacian to G_t and U_t because they should be spatially continuous.
4. After solving R_t, S_t, G_t and U_t for each trace, we will divide all traces by their corresponding R_t, S_t and G_t to remove the artifacts.

Extract AVA attributes and evaluate their variability

After amplitude balancing, we perform split-step phase shift migration and extract multiple angle gathers from the image using multiple equal-probable velocity models. Then we follow Gratwick's algorithm (Gratwick, 2001) to get intercept and gradient. After extracting intercept

A and gradient B from angle gathers, we first cross-plot A and B (Ross, 2000; Castagna and Swan, 1997) and muted those clusting points in the plots which correspond to background values. Then we transformed the muted plots back to two panels A and B. A negative A*B value often is a hydrocarbon indicator. The variability of AVA attributes can be assessed by comparing and contrasting their multiple realizations. A convenient way to analysis the variability is to use histogram. Because the count used here is the function of CMPX, depth and magnitude of AVA attributes, the histogram used here is a 3-D cube.

THE SEISMIC DATA AND THE WELLS

The land seismic data used in this paper is from South America. In CMPX-CMPY coordinate, the CMPX range of seismic data is approximately from 1.65km to 5.8km and CMPY is approximately from 0.375km to 7.925km.

There are about 30 wells drilled in this area. Some of them are productive, some are moderately productive and one is dry. Most of the wells have spontoneous-potential, resistivity, gamma ray and sonic logs. Some wells have density and neutron logs.

Figure 1 shows the well locations in this area. The straight line is where we will extract seismic amplitude information. The line was chosen by matching the wells A, B and C using linear least square method, resulting in coordinate as cross-line=106.33 (CMPY=2.225km). Table 1 is the detailed information of the coordinates of three wells used to match the line.

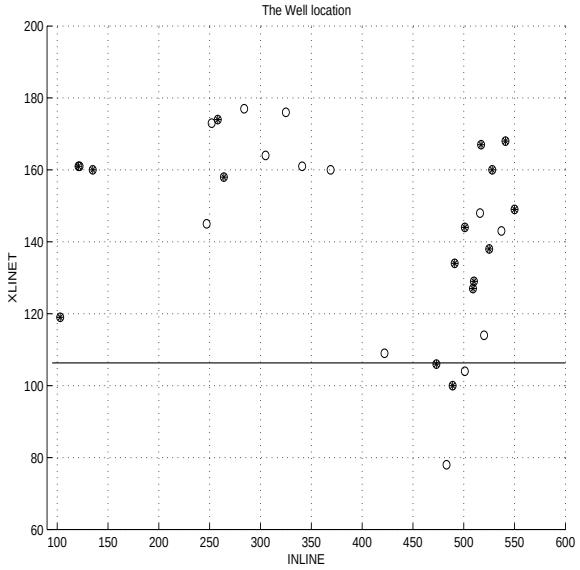

Figure 1: The well locations and the 2-D line along which we performed velocity analysis. chen-wellloc [CR]

Table 1: The coordinates of the wells

Well	Inline	Crossline	CMPX	CMPY
Well A	501	104	3.875km	2.125km
Well B	422	109	5.375km	2.375km
Well C	473	106	4.575km	2.225km

The wells don't lie exactly along the line. The cross-line distance between the line and the well A, B and C are 100m, 150m and 0 respectively. We assume the rock properties don't change rapidly across these small spans.

TRADITIONAL RESULTS

The gamma ray log is one of the most reliable logs. The well A, B and C have different depth ranges for the gamma ray log. Table 2 shows the depth range of the gamma ray log of these three wells. The depth origin is at surface, which is same as that for seismic data.

Table 2: The gamma ray log interval of the wells

Well	log start	log end
Well A	3.117 km	3.577 km
Well B (Part1)	2.033 km	2.570 km
Well B (Part2)	3.100 km	3.580 km
Well C	1.831 km	3.599 km

The gamma ray log is most frequently used to quantify shale volume along the well (Rider, 1996). According to the consolided condition of rock property in this area, we used following empirical equation (Atlas, 1992) to calculate shale volume from gamma ray value:

$$V_{shale} = 0.33\left(2^{2V^*_{shale}} - 1\right) \tag{6}$$

Here V^*_{shale} is the linear function of γ:

$$V^*_{shale} = \frac{\gamma - \gamma_{min}}{\gamma_{max} - \gamma_{min}} \tag{7}$$

The γ here is the gamma ray value, γ_{min} and γ_{max} are the minum and maximum value of the gamma ray. Figure 2 show the gamma ray log of these three wells. Figure 3 is the shale volume calculated by using equation (6).

RESULTS OF VARIABILITY STUDY

The scatterplot between AVA attributes and shale volume

We extracted AVA attributes (intercept, gradient, and their product) at three well locations: CMPX=3.875km for well A, 5.375km for well B and 4.575km for well C. The well log has much higher vertical resolution than seismic data, so, in order to correlate the AVA attributes and log data at same depth, we used sinc function to interpolate the log data. I applied the same depth window that ranges from 3.12 km to 3.57 km for the three wells and scatterploted AVA attributes and shale volume. Figure 4 show the result. We can't see obvious correlation

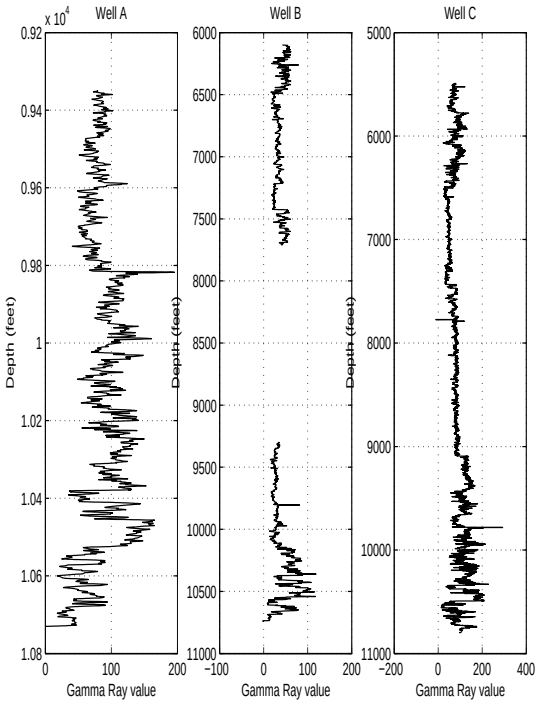

Figure 2: From left to right are the gamma ray log for the well A, B and C chen-gammaray [CR]

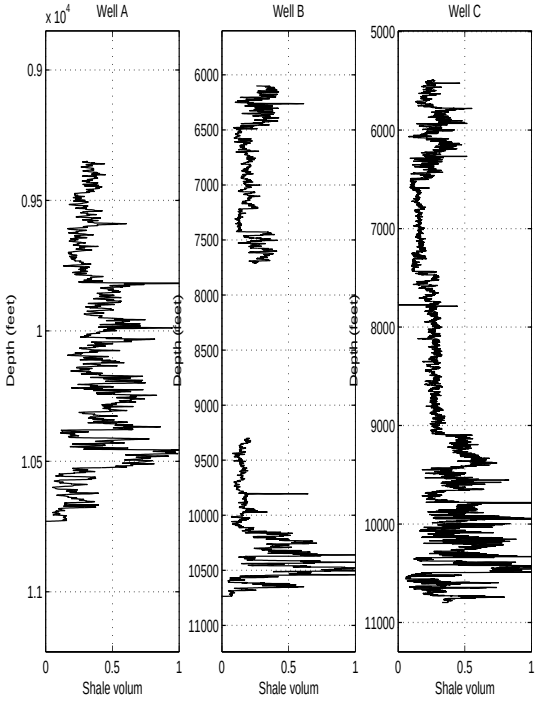

Figure 3: From left to right are the shale volume for the well A, B and C. The shale volume was calculated from gamma ray value using equation (6). I selected γ_{max} for A,B and C as 165,105 and 200 respectively by hand chen-shaleline1 [CR]

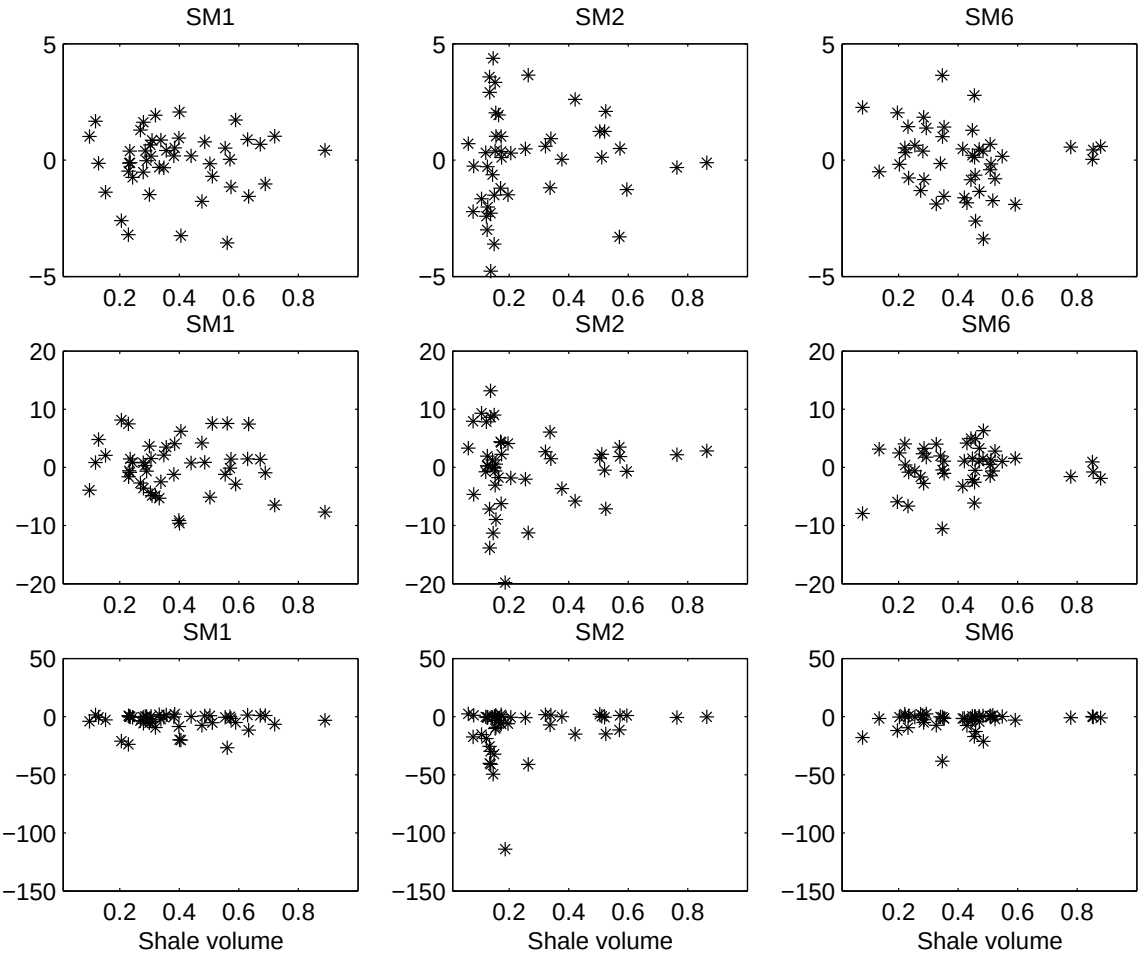

Figure 4: Scatterplot between AVA attributes and shale volume. From left to right, the column is for well A, B and C, respectively; from up to bottom, the y-axis is intercept, gradient and their product respectively. The x-axis is shale volume for all of them. chen-scatter [CR]

between AVA attributes and shale volume in this figure, but we can tell that the shale volume in the depth window along well B has a much lower value than other two wells.

Theoretically, AVA attributes will correlate better with impedance rather than shale volume. Unfortunately, we didn't have density log for well A and B. We scatterploted velocity from sonic log and AVA attributes for all three wells. We didn't see any positive caused high AVA uncertainty here.

The uncertainty of AVA attributes along the wells

We generated the histogram cube by using 50 multiple realizations. From the histogram, we found the AVA attributes along well B have obviously bigger avearage uncertainty than well A and well C in the depth range we studied. Figure 5 and Figure 6 show the depth slice at

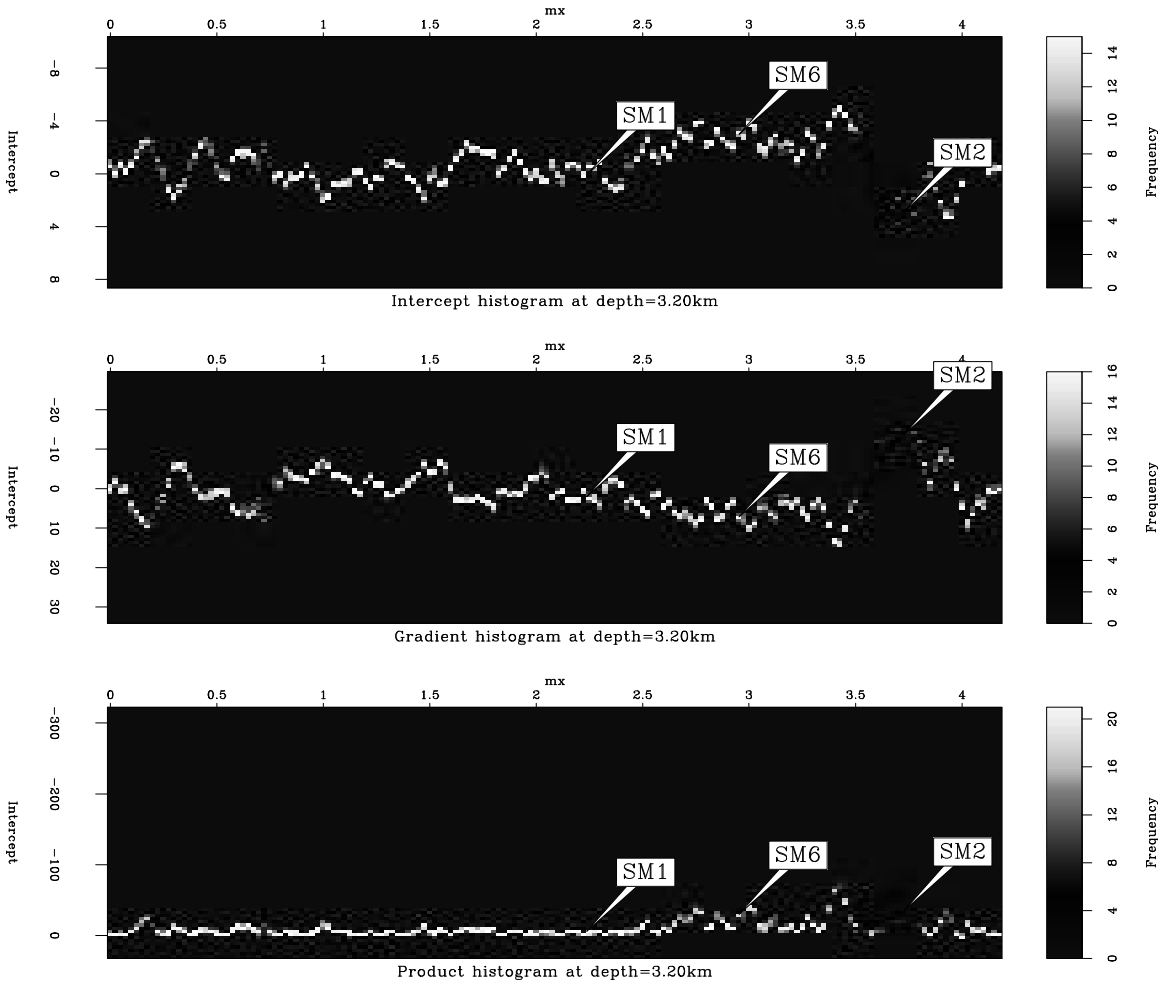

Figure 5: The depth slice of histogram cube at 3.20km. The origin of CMPX in this plot is at CMPX=1.65km chen-320.ann [CR]

3.20km and 3.43km respectively from histogram cube. The low shale volume along the well B in the depth window make us guess the low shale shale/sand ratio causes hig AVA uncertainty here.

CONCLUSION

Using a dataset from South America, we generated a 3-D histogram to conveniently evaluate the uncertainty of AVA attributes in this area. The variability of the AVA attributes was assessed using the multiple realizations method developed by Clapp (2002). From the gamma ray log we found the well with low shale volume has high AVA uncertainty, which made us guess the low shale/sand ratio may cause high AVA uncertainty. Further work should be done using more real data to explore empirical relationships between AVA uncertainty and rock information, such as shale/sand ratio, impedance or velocity.

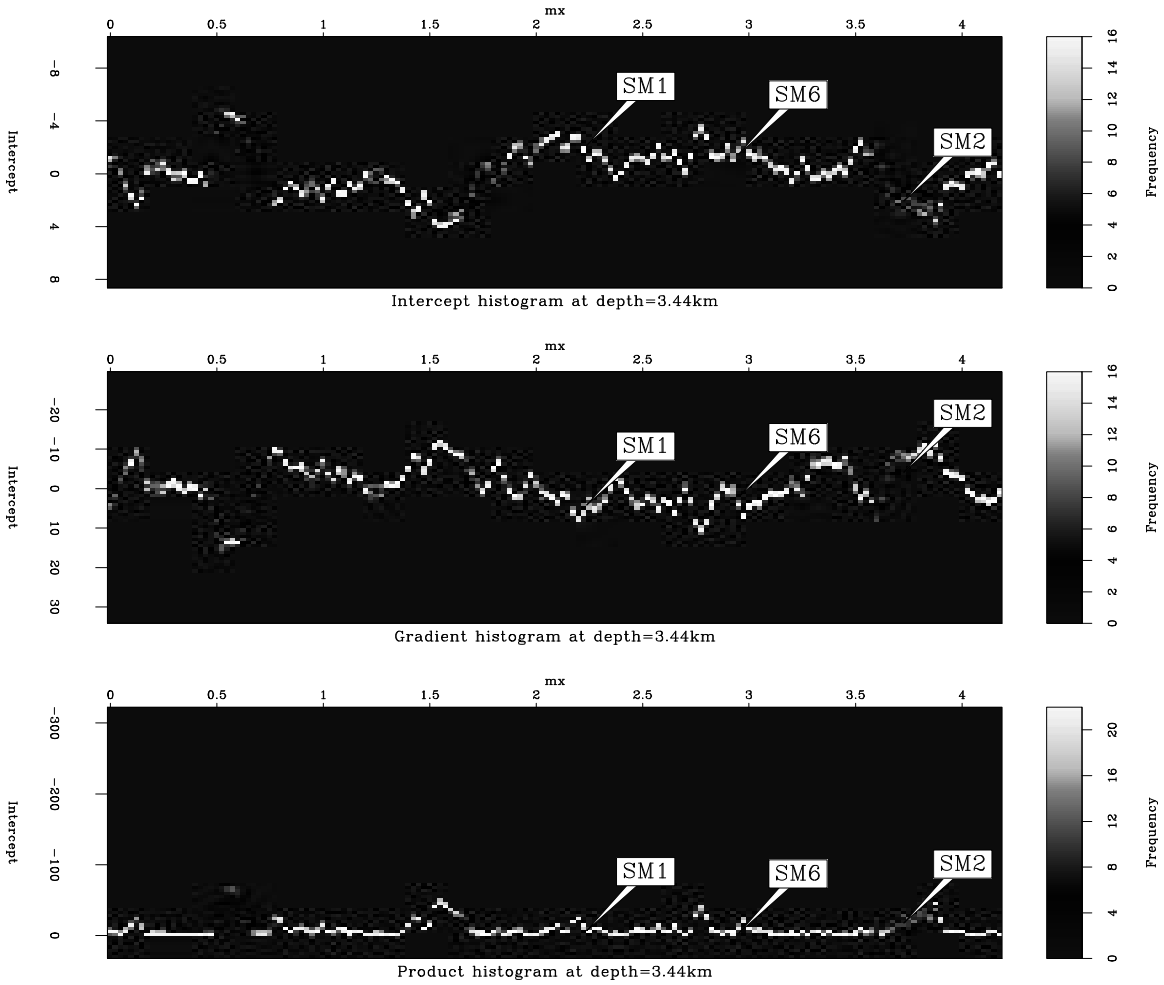

Figure 6: The depth slice of histogram cube at 3.43km. The origin of CMPX in this plot is at CMPX=1.65km chen-343.ann [CR]

ACKNOWLEDGMENTS

We would like to thank the company who provided the data used in this paper; to Andres Mantilla and Tapan Mukerji for their helpful discussions; and to the SEP group for their overall support.

REFERENCES

Atlas, 1992, Digital circumferential borehole imaging log: Western Atlas International.

Castagna, J. P., and Swan, H. W., 1997, Principles of AVO crossplotting: AAPG Mid-Continent Section Meeting; Abstracts; AAPG Bulletin, **81**, 1348.

Castagna, J. P., 1993a, Avo analysis - tutorial and review: Offset-dependent reflectivity - Theory and practice of AVO analysis.

Castagna, J. P., 1993b, Rock physics - the link between rock properties and avo response: Offset-dependent reflectivity - Theory and practice of AVO analysis.

Claerbout, J., 1999, Geophysical estimation by example: Environmental soundings image enhancement: Stanford Exploration Project, `http://sepwww.stanford.edu/sep/prof/`.

Clapp, R., 2000, Multiple realizations using standard inversion techniques: SEP–**105**, 67–78.

Clapp, R. G., 2001, Multiple realizations: Model variance and data uncertainty: SEP–**108**, 147–158.

Clapp, R. G., 2002, Effect of velocity uncertainty on amplitude information: SEP–**111**, 255–269.

Gratwick, D., 2001, Amplitude analysis in the angle domain: SEP–**108**, 45–62.

Isaaks, E. H., and Srivastava, R. M., 1989, An Introduction to Applied Geostatistics: Oxford University Press.

Mora, C., and Biondi, B., 2000, Estimation of AVO attributes sensitivity to velocity uncertainty using forward modeling: A progress report: SEP–**103**, 349–366.

Rider, M., 1996, The geological interpretation of well logs: Gulf Publishing Company.

Ross, C. P. Effective AVO crossplot modeling: A tutorial:, 2000.